P1.2

THE IMPACT OF THE SURFACE HETEROGENEITY ON THE ENERGY IMBALANCE PROBLEM USING LES

Atsushi Inagaki*, Marcus Oliver Letzel**, Siegfried Raasch** and Manabu Kanda*
* Tokyo Institute of Technology, Tokyo, Japan
** University of Hannover, Hannover, Germany

1. INTRODUCTION

The variety of ground conditions or a partially cloud covered surface can cause a differential surface heating and make a strong impact on the atmospheric boundary layer (ABL) flow statistics. We investigated the influence of such a heterogeneous surface conditions on the vertical heat transport process, especially focusing on the surface energy budget based on a single point observation.

The recent study has reported that the fluxes measured using eddy covariance (EC) at the point observations underestimate the surface energy budget (i.e. Lee and Black, 1993), which are called energy imbalance problem. Concerning this problem, Kanda et al. (2004) revealed the systematical error included in EC method theoretically and numerically over a horizontally homogeneous surface condition. The main difference between the present study and the homogeneous one is an occurrence of the mesoscale circulations invoked by surface heterogeneity, which can modify the CBL structure strongly. Based on the previous study (Kanda et al., 2004), we evaluated the horizontal representativeness of a single point measurement over an idealized heterogeneous area with numerical approach, where the horizontal heterogeneity is imposed on the ground heating as one-dimensional sinusoidal alternation.

2. THEORETICAL BACKGROUND

Some assumptions are applied in the present study. The vertical ascending and descending flow balances in the total domain at every time step, the ground surface is completely flat and no horizontal mean flow exists. The heat flux supplied from the ground spatially alters but it is temporally constant.

2.1 *Turbulent Fluxes and Mesoscale Transport*

We use two kinds of turbulent heat fluxes to evaluate the vertical heat transport process. One is defined as the deviation from the temporal average which represents an EC flux based on the tower observation. Another is defined as the deviation from the phase average which is averaged over the same portion in each phase. The comparison of these two kinds of fluxes allows us to evaluate the spatial representativeness of the point observation over the heterogeneous surface region.

The local kinetic vertical heat flux (hereafter, vertical heat flux) at the surface of measurement height (100 m above the ground) is expressed as,

$$F = wT \tag{1}$$

where w and T are vertical velocity component (m s^{-1}) and potential temperature (K) respectively. These variables can be decomposed into a mean and a deviation using two different methods, which are temporal average at each observation point or instantaneous phase average along the surface pattern. These are shown in Eqs.(2a), (2b),

$$w = \overline{w} + w_t', \quad T = \overline{T} + T_t' \tag{2a}$$

$$w = [w]_p + w_p', T = [T]_p + T_p' \tag{2b}$$

Here ($\bar{}$) is the temporal average, and ($[]_p$) is the phase average. Superscript (') means the deviation, and subscripts ($_t$) and ($_p$) distinguish temporal or phase deviation.

Substituting Eqs.(2a), (2b) into Eq.(1) with temporal or phase averaging respectively, the following equations are derived,

$$\overline{F} = \overline{w}\,\overline{T} + \overline{w_t' T_t'} \tag{3a}$$

$$[F]_p = [w]_p [T]_p + [w_p' T_p']_p \tag{3b}$$

The relations of $\overline{w_t'} = \overline{T_t'} = [w_p']_p = [T_p']_p = 0$ are used here. The third term of Eq.(3a) is used in conventional tower observation. And we define the second term of Eq.(3b) as the mean heat transport due to the mesoscale circulation (hereafter, mesoscale heat flux). Now especially denote about the homogeneous case, this mesoscale mean transport $[w]_p [T]_p$ must become zero because there is no horizontal variation on the ground. Therefore the phase averaged vertical velocity corresponds to the horizontal area averaged one which is always zero from the assumption of no synoptic vertical flow. This strictly satisfies that there is no mesoscale heat flux in the homogeneous case.

* *Corresponding author address*: Atsushi Inagaki, Tokyo Institute of Technology, Dept. of International Development Engineering, Meguro-ku, O-okayama, 2-12-1 Tokyo, 152-8552 JAPAN; e-mail: inagaki@ide.titech.ac.jp

2.2 *Definition of Imbalance*

In the present study, we define the imbalance of surface energy budget excluding the contribution of the mesoscale circulation on the net vertical heat transport. It is because the locally constant up/down-draft is systematically excluded from the point EC measurement, which is represented as the mesoscale heat flux in the present study. Furthermore, the estimation of the net effect of such mesoscale flow is beyond the scope of the point observation. So that it is useful to evaluate the point observation subtracting the effect of mesoscale mean transport from the domain averaged flux. The formula represents this imbalance appears in Sec.4.2 (Eq.5).

3. EXPERIMENTAL DESIGN

LES is just the tool to address this problem because of its ability to represent turbulent organized structures (TOS). PALM (PArallelized Large eddy simulation Model) developed by Raasch and Schröter (2001) has been used for the present study. PALM solves the Navier-Stokes equations for a Boussinesq fluid, the first law of thermodynamics and the equation for turbulent kinetic energy (TKE). Subgrid-scale (SGS) turbulence is parameterized according to Deardorff (1980) with minor change. Non-divergence is assured at every time step by solving a Poisson equation for pressure. Cyclic conditions apply at the lateral boundaries. Monin-Obukhov similarity is assumed in the Prandtl layer between the ground surface and the first computational grid level. The roughness length is constant (0.1 m). Gravity waves are damped out from 1,800 m above the ground level.

The three dimensional domain size is 16 x 16 x 2.7 km, grid spacing is 50 m for each direction. The initial temperature profile is set 0.8 K km^{-1} up to a height of 1,200 m and 7.4 K km^{-1} aloft for a strong capping inversion, which assumes a typical daytime ABL. The ground is completely flat but has inhomogeneous properties represented as heterogeneous heat flux supply with one-dimensional sinusoidal alternation,

$$F_{gv} = F_g + F_g A \sin\left(\frac{2\pi}{\lambda} x\right) \quad (4)$$

where F_{gv} is the ground surface heat flux at location x in the x-direction (K m s^{-1}). λ is wavelength (m), A is amplitude (%) of surface perturbation. F_g is the mean heat flux over the ground level. The present study uses a fixed value of F_g = 0.1 (K m s^{-1}) in all simulations. The measurement height is selected 100 m above the ground where the energy budget is analyzed. The summary of the experimental conditions are listed in the Table 1.

Table 1 Summary of experimental conditions

Case	λ (km)	A (%)	Case	λ (km)	A (%)
Case0	0	0	Case2−4	2	40
Case1−2	1	20	Case2−8	2	80
Case1−4	1	40	Case8−2	8	20
Case1−8	1	80	Case8−4	8	40
Case2−2	2	20	Case8−8	8	80

λ : wavelength (km), A : amplitude (%)

4. RESULTS

4.1 *Mesoscale Mean Vertical Heat Transport*

At first we investigate the net vertical heat transport due to the mesoscale circulation using the correlation term of the phase mean variables ($[w]_p[T]_p$) with the temporal and total domain average. When the wavelength is 2 km or more, this mesoscale heat flux becomes larger and larger with the increase of amplitude, which reaches about 25 % of the domain average in the 80 % amplitude cases (Fig.1). In contrast, those of the 1 km wavelength cases are hardly enhanced by stronger heat amplitudes, which are less than 5 % even in the 80 % amplitude case. Instantaneous vertical velocity maps are shown in Fig.2 for 1 km and 8 km wavelength and same amplitude of surface heating, which depict only a representative quarter of the whole domain (8 x 8 km) for better visibility. Fig.2a shows that the 1 km wavelength doesn't develop a mesoscale circulation that clearly corresponds to the pattern of the surface heterogeneity. Then the turbulent organized structures (TOS) become similar to that of homogeneous surface case so that the phase averaged vertical velocities and the mesoscale mean heat flux becomes near zero at any location. In contrast, the longer wavelength cases (more than 2km) develop the flow structures along the surface pattern (Fig.2b), which enhance the characteristics of phase mean variables. The minimum horizontal scale of mesoscale circulations is determined by the BL height (Shen and Leclerc, 1995), which becomes about 1.4 km in these simulations so that the 1 km wavelength is too small to develop a clear mesoscale flow structure.

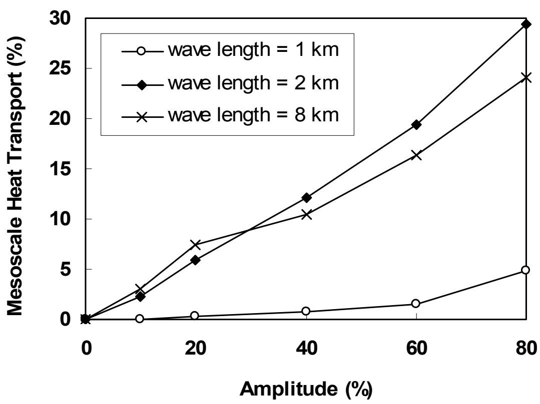

Fig.1 Mesoscale mean heat transport

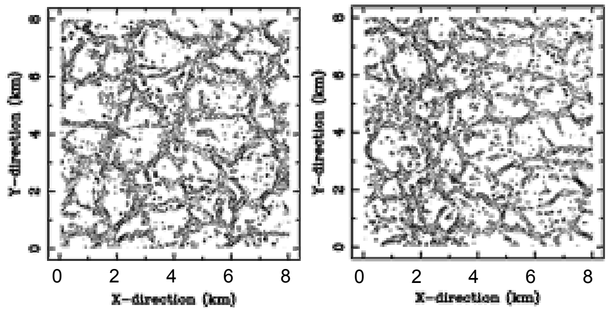

(a) wavelength: 1 km (b) wavelength: 8 km

Fig.2 Instantaneous vertical velocity maps (amplitude: 40 %, only depict updraft region)

4.2 *Phase Representativeness of EC Method*

To evaluate the surface budget based on the temporal EC method excluding the effect of mesoscale heat transport, we define the imbalance (hereafter, phase imbalance I_p) in phase as follow,

$$I_p = \overline{[w_t' T_t']}_p - ([\bar{F}]_p - \overline{[w]_p [T]_p})$$
$$= \overline{[w_t' T_t']}_p - \overline{[w_p' T_p']}_p \qquad (5)$$

Fig.3 shows this phase imbalance normalized by the temporal and total domain averaged vertical heat flux. It is found that the turbulent flux estimated by temporal averaging in the point measurement is always less than this surface energy budget in all cases even excluding the heat transport due to the mesoscale circulations. The maximum of this negative bias occurs mostly at the crest of the surface perturbation where the phase coordinate x is, (top) 0.25, (middle) 0.5, (bottom) 2 in Fig.3 respectively. The minimum bias appears at the trough although these features are not so clear in the weak surface perturbation cases (amplitude = 20 %) or smaller wavelength cases (wavelength = 1 km).

In the 2 km or 8 km wavelength cases, the more the surface heat amplitude increases, the more this negative deviation approaches to zero over the trough part of surface perturbation. Over the crest, the magnitude of negative bias changes little and arises to a relatively large value independent of the amplitude.

Kanda et al. (2004) revealed that a lack of energy budget based on a point measurement is due to the net vertical heat transport effect of thermal organized structure (TOS). In case of the present study, the effect of TOS developed according to the surface pattern is mostly included in the mesoscale heat flux represented as phase average (Eq.3b). While, the effect of remainder TOS is excluded from both the mesoscale transport and the EC turbulent flux, so it becomes phase imbalance. The latter structures appear mostly over the weak heating area (Fig.2) and develop perpendicular to the surface pattern which is x-direction in the present study.

There are two possibilities for the decrease of the magnitude of phase imbalance over a trough of surface perturbation with increase of ground heat amplitude (Fig.3).

One is that the flow structure over the trough of surface heat becomes weak. Fig.4 shows the instantaneous vertical velocity maps with 20 % and 80 % amplitude and same wavelength (8 km). Compared with these two and 40 % amplitude case (Fig.2b), the flow structure over the weakly heated area (near around x = 6 km) becomes much weaker in the 80 % ground heat amplitude case. The large amplitude creates a strong horizontal pressure gradient so that the randomly distributed vertical eddies like structures developed perpendicular to the surface heterogeneity organize in rolls (Avissar and Schmidt, 1998). The updraft structures appear over the trough of surface heating is mostly different from mesoscale flow structure so that the decreases of its magnitude cause the decrease of phase imbalance.

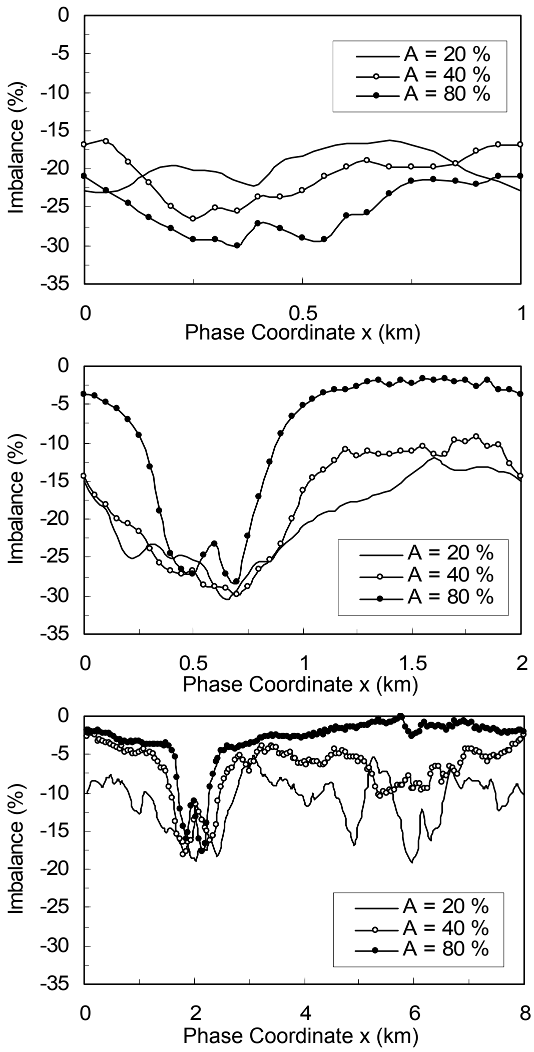

Fig.3 Imbalance over the heterogeneous surface in phase normalized by the domain averaged flux (top) λ =1 km, (middle) λ =2 km, (bottom) λ =8 km

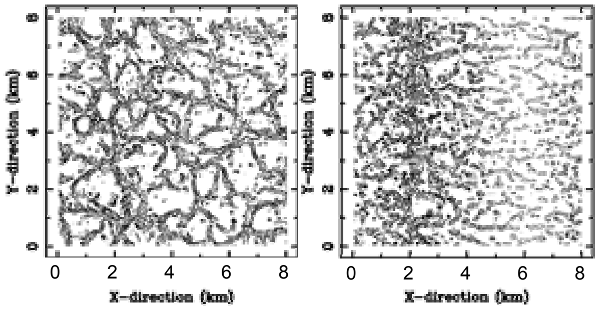

(a) amplitude: 20 %   (b) amplitude: 80 %

Fig.4 Instantaneous vertical velocity maps
(wavelength: 8 km, only depict updraft region)

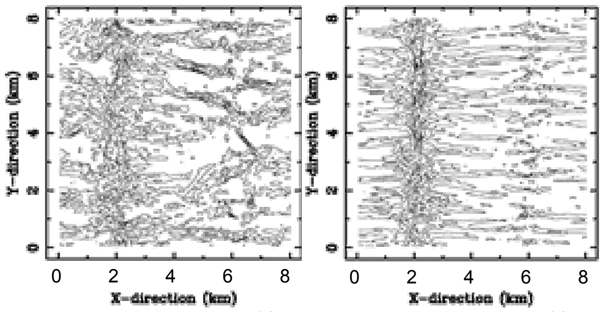

(a) amplitude: 40 %   (b) amplitude: 80 %

Fig.5 1-hour averaged vertical velocity maps
(wavelength: 8 km, only depict updraft region)

Over the crest of surface heating (Fig.2b and 5, near around x = 2 km), the flow structure isn't weakened by strong amplitude and creates the rich variation of vertical flow structure along y-direction. Although the flow characteristics after phase average is reflected in the mesoscale heat flux, the rich variations of TOS along y-direction enhance the phase imbalance. This explains the constantly large negative bias of the phase imbalance.

Another possibility comes from the movement of the individual TOS over a trough of the surface perturbation that are embedded in the mesoscale circulation flow. Over the trough area, the strong horizontal heterogeneity increases the horizontal wind speed in the direction of the surface perturbation (x-direction) (Avissar and Schmidt, 1998), and it advects the TOS faster and faster. So after temporal average, the TOS over the trough becomes weak (Fig.5). Thus the phase imbalance decreases over the trough. The TOS over the crest area is more stationary for any surface amplitude and isn't so weakened after temporal averaging.

In the 1 km wavelength, the TOS pattern isn't stationary but evenly distributed in the entire domain (Fig.2a). This TOS pattern is seldom weakened and the embedded flow to the TMC doesn't appear for the strong amplitude. Thus these evenly distributed structures arise the phase imbalance, not enhance the mesoscale mean transport. Then the phase imbalance is always constantly large at any location.

4. CONCLUSION

We investigated the net heat transport by the mesoscale circulation invoked by the heterogeneous surface conditions using phase averaging in an idealized heterogeneous domain and revealed that its transport contribution is not small compared to the total domain heat flux when a clear mesoscale circulation develops.

This heat transport process is mostly neglected in the EC method so that we evaluated the surface energy budget using EC method excluding the mesoscale heat transport contribution. Even then the EC point measurement still underestimates the surface energy budget. However, that shortage gets close to zero when a strong mesoscale circulation exists. This underestimate is mainly attributed to the temporal mean TOS developed perpendicular to the primary mesoscale flow structure, which becomes weak when the horizontal heterogeneity is strong.

ACKNOWLEDGEMENTS

This research was supported by CREST (Core Research for Evolution Science and Technology) of JST (Japan Science and Technology cooperation) and by a Grant-in-Aid for Developmental Science Research from the Ministry of Education, Science and Culture of Japan.

REFERENCES

Avissar, R. and Schmidt, T., 1998: An Evaluation of Scale at which Ground-surface Heat Flux Patchiness Affects the Convective Boundary Layer Using Large-Eddy Simulations, J. Atmos. Sci., **55**, 2666–2689.

Deardorff, J.W., 1980: Stratocumulus-topped mixed layers derived from a three-dimensional model, Boundary-Layer Meteorol., **18**, 495–527.

Kanda, M., Inagaki, A., Letzel, M.O., Raasch, S., Watanabe, T.,2004: Les study of the energy imbalance problem with eddy covariance fluxes, Boundary-Layer Meteorol., **110**, 381-404.

Lee, X. and Black, T. A., 1993: Atmospheric Turbulence within and above a Douglas-Fir Stand. Part2: Eddy Fluxes of Sensible Heat and Water Vapour, Boundary-Layer Meteorol., **64**, 369–389.

Letzel, M.O. and Raasch, S., 2003: Large-Eddy Simulation of Thermally Induced Oscillations in the Convective Boundary Layer. J. Atmos. Sci., **60**, 2328-2341.

Raasch, S. and Schröter, M., 2001 : PALM - A large-eddy simulation model performing on massively parallel computers. Meteorol. Z., **10**, 363-372.

Shen, S. and Leclerc, M.S., 1995: How Large Must Surface Inhomogeneities be Before They Influence the Convective Boundary Layer Structure? A Case Study, Q. J. R. Meteorol. Soc., **121**, 1209-1228